SIMULATION OF SEMICONDUCTOR DEVICES AND PROCESSES Vol. 4
Edited by W. Fichtner, D. Aemmer - Zurich (Switzerland) September 12-14, 1991 - Hartung-Gorre

Physical modelling and performance evaluation of III-V heterostructure avalanche photodiodes

David Tammaro, Augusto Benvenuti
Politecnico di Torino, Dipartimento di Elettronica,
Corso Duca degli Abruzzi 24, 10129 Torino, Italy

Giovanni Ghione
Università di Catania, D.E.E.S.,
Viale Andrea Doria 6, Catania, Italy

Abstract

A physical simulator of heterostructure avalanche photodiodes (APD's) for optical communications is discussed. The simulator is based on a 1D drift-diffusion two-carrier model allowing for heterojunctions, Fermi statistics, optical, avalanche and SRH G-R mechanisms. Particular care is devoted to the implementation of local avalanche models, which have a great impact on the performance evaluation of this device class both from the standpoint of signal and of the excess noise behaviour. Preliminary results are presented on the DC behaviour of state-of-the-art APD's.

1 Introduction

Heterostructure avalanche photodiodies (APD's) are today among the most promising photodetectors for optical communication systems. Owing to their complex, multilayered structure, the design and optimization of heterostructure APD's would greatly benefit from a physical simulator able to accurately evaluate the device performances from material data and geometry.

The physical simulation of photodiodes has been sparsely addressed in the literature during the past years. While the microscopic photodetection mechanisms have been the object of extensive investigation, device simulation was mainly restricted to *p-i-n* structures or Schottky photodiodes: see e.g. [9], [14] for a Monte Carlo model, [8] and [2] for a drift-diffusion, time-domain model. Concerning APD's, the simulation is made more complex by the presence of avalanche ionization (see within this context [18, 19]) and, in most state-of-the-art devices, of heterojunctions. The simulation of heterostructures with heavily doped materials has been discussed in [11, 12, 22],. Device simulation studies have been made for InGaAs APD's in [17], while [16] exploits a hybrid computation technique to investigate the frequency response of $Al_xGa_{1-x}As$ and $In_xGa_{1-x}As$ APD's.

The design and performance assessment of APD's is based upon a few figures of merit which can be derived from DC analysis. These are the inverse current under dark and under illumination, as a function of the incident optical power, and the excess shot noise generated by the detector. The large-signal behaviour under optically pulsed operation, which is not investigated in the present paper, is also relevant to system design, since it yields the time delay introduced by the detector.

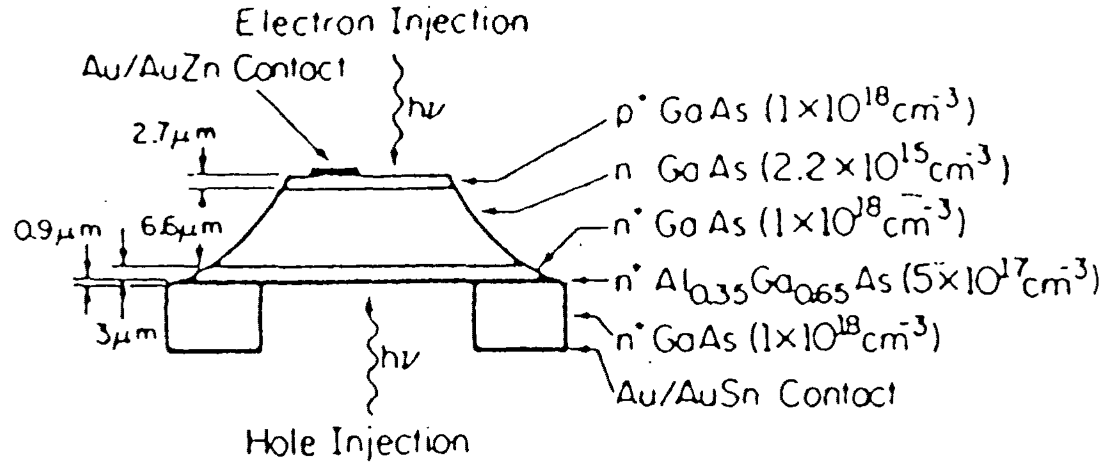

Figure 1: p^+-n AlGaAs/GaAs photodiode [3].

The paper is structured as follows. Sec.1 introduces the physical model used for simulation. Numerical issues are discussed in Sec.2, while Sec.3 is devoted to presenting preliminary results on the two state-of-the-art homo- and heterostructure APD's shown in Fig.1 and Fig.2.

2 The physical model

The physical model implemented is a one-dimensional, two-carrier drift-diffusion model allowing for abrupt and graded heterostructures and Fermi-Dirac statistics [11, 12]. The model equations read in steady-state DC conditions:

$$\nabla^2\psi = -\frac{q}{\epsilon_s}(p - n + \sum_j N_{Dj}^+ - \sum_i N_{Ai}^-) \tag{1}$$

$$\nabla\cdot\underline{J}_n = qR \tag{2}$$

$$\nabla\cdot\underline{J}_p = -qR \tag{3}$$

where:

$$\underline{J}_n = q[n\mu_n(\mathcal{E})\underline{\mathcal{E}} + D_n(\mathcal{E})\nabla n - n\mu_n\nabla\chi - n\mu_n V_T\nabla\log N_C], \tag{4}$$

$$\underline{J}_p = q[p\mu_p(\mathcal{E})\underline{\mathcal{E}} - D_p(\mathcal{E})\nabla p - p\mu_p\nabla(\chi + E_g) + p\mu_p V_T\nabla\log N_V] \tag{5}$$

are the electron and hole current densities. n is the electron density, p the hole density, $\underline{\mathcal{E}}$ the electric field, ψ the potential, μ_n, μ_p, D_n, D_p the mobility and diffusivity of electrons and holes, respectively; χ is the semiconductor affinity, $V_T = kT/q$, and N_V, N_C the effective densities of states in the valence and conduction band. Finally, N_{Dj}^+ is the density of the ionized j-th donor, N_{Ai}^- the density of the ionized i-th acceptor:

$$N_{Ai}^- = N_{Ai}\frac{c_{ni}n + c_{pi}n_i\exp(-a)}{c_{ni}[n + n_i\exp(a)] + c_{pi}[p + n_i\exp(-a)]} \tag{6}$$

$$N_{Dj}^+ = N_{Dj}\frac{c_{pj}p + c_{nj}n_i\exp(d)}{c_{nj}[n + n_i\exp(d)] + c_{pj}[p + n_i\exp(-d)]} \tag{7}$$

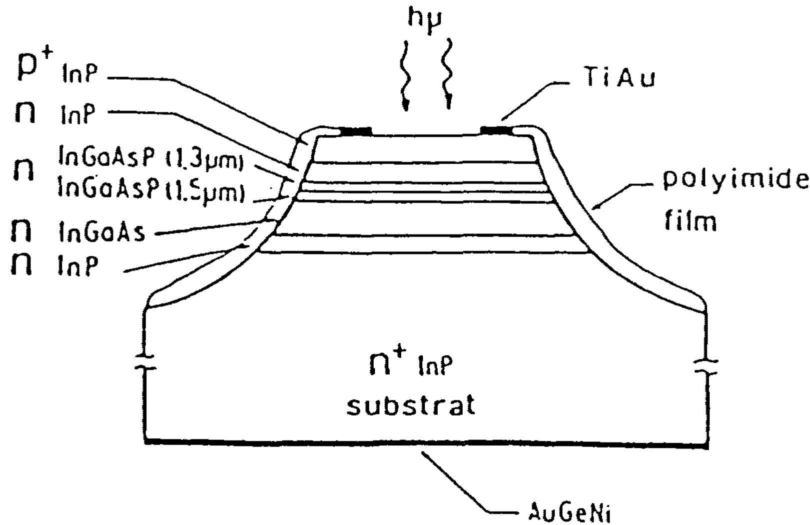

Figure 2: SAM-APD InP/InGaAsP/InGaAs photodiode [4].

where:

$$a = \frac{\Delta E_V - 0.5[E_g + kT\log(N_C/N_V)]}{kT}, \quad d = \frac{0.5[E_g + kT\log(N_C/N_V)] - \Delta E_C}{kT}. \quad (8)$$

E_g is energy gap of the material, k the Boltzmann constant, T the lattice temperature. Donor and acceptor levels are characterized by the concentration N_A or N_D, the activation energy, given by the energy difference between the impurity level and the bottom of the conduction band, ΔE_C, for donors, or by the energy difference between the impurity level and the top of the valence band, ΔE_V, for acceptors, and the capture probabilities c_n, c_p.

The net recombination rate $R = U - G$ where G and U are the generation and recombination rates, respectively, includes Shockley-Read-Hall RG, optical generation and avalanche generation. Avalanche generation is omitted from the model in the analysis of p-i-n photodiodes.

The optical generation coefficient has the following expression:

$$G_o(x) = \eta\frac{P}{Ah\nu}(1 - R)\exp(-\eta x) \quad (9)$$

where η is the absorption coefficient, A the device cross-section, h the Planck constant, ν the frequency of the optical signal, P the optical power, and R the reflection coefficient of the device surface. Avalanche generation is expressed in the usual form:

$$G_a(x) = \frac{1}{q}(\alpha_n \mid J_n \mid + \alpha_p \mid J_p \mid). \quad (10)$$

The models for the ionization coefficients α_n, α_p require a more detailed discussion. Modelling the impact ionization means evaluating the probability that the carriers (electrons and holes) gain from the external field an energy equal or greater than the ionization threshold energy E_i. Most *local* theories, in which the ionization coefficients only depend on the local electric field $\mathcal{E}(x)$, originate from two classical models: Wolff's diffusion model [24], in which the impact ionization coefficients have the form $\alpha \propto \exp(-b/\mathcal{E}^2)$, where b is a constant and $\mathcal{E}$ is

the electric field, and Shockley "lucky electron" model [20] in which $\alpha \propto \exp(-E_i/ql\mathcal{E})$, where l is the mean free path. The first and second model yields a good fitting to experiment for high and low fields, respectively. Using Baraff's approach [1], Thornber developed an approximation which attempts to link Wolff and Shockley models. Thus, the following models for the electron impact ionization rate have been implemented in the simulator:

- The Thornber-Baraff formula [1]:

$$\alpha_n(\mathcal{E}) = \frac{q\mathcal{E}}{E_i} \exp\left(\frac{-\mathcal{E}_{if}}{\mathcal{E}(1+\frac{\mathcal{E}}{\mathcal{E}_t}) + \mathcal{E}_{kT}}\right) \tag{11}$$

  where $\mathcal{E}_{if}$, $\mathcal{E}_t$, and $\mathcal{E}_{kT}$ are the fields for which the carriers reach the ionization threshold energy, the optical phonon energy, the thermal energy kT, respectively, in one mean free path. Wolff diffusion model [24] and Shockley "lucky electron" model [20] can be considered as particular cases of the Thornber-Baraff approach.

- The Chynoweth model [7]:

$$\alpha_n(\mathcal{E}) = \alpha_n^{\infty} \exp\left(-\frac{b_n}{|\mathcal{E}|}\right) \tag{12}$$

  where α_n^{∞} and b_n are fitting parameters, and Lackner's modification [10]:

$$\alpha_n(\mathcal{E}) = \frac{1}{L_n} \frac{\exp\left(-\frac{E_{in}}{qL_n\mathcal{E}}\right)}{1 + \frac{E_{in}}{qL_n\mathcal{E}} \exp\left(-\frac{E_{in}}{qL_n\mathcal{E}}\right) + \frac{E_{ip}}{qL_p\mathcal{E}} \exp\left(-\frac{E_{ip}}{qL_p\mathcal{E}}\right)} \tag{13}$$

  where the input parameters are the mean free paths L_n, L_p and the threshold energies E_{in}, E_{ip}.

Similar models are adopted for the hole impact ionization rate. For the physical parameters implemented in the models, see [5, 15] and references therein for binary compounds and III-V semiconductor alloys, respectively.

Non-local models for impact ionization, though potentially more accurate and correct than local models, require a physical model in which the history of the carriers is described, either completely, as in Monte Carlo models, or at least on average, as in energy-transport (hydrodynamic) models. Nevertheless, even within the framework of a drift-diffusion model a non-local theory such as the "modified lucky drift theory" first proposed by Childs [6] can be implemented, at least in a non-selfconsistent manner.

Concerning the noise properties of the avalanche photodiode, a simplified treatment proposed by McIntyre [13] allows the noise power density to be derived from the hole distribution along the optical signal propagation direction. Such approach allows a straightforward implementation within the framework of a 1D drift diffusion model. Details on non-local and noise models will be provided in an extended version of the paper.

3 Simulation

The implementation of the DC physical model was performed in one dimension through a central finite-difference discretization which extends the well-known Scharfetter-Gummel scheme. The current densities at midpoints are approximated as:

$$J_n^{i+1/2} = \frac{q\mu_n^{i+1/2}V_T}{h_i}[B(\Delta_n^{i+1/2})n_{i+1} - B(-\Delta_n^{i+1/2})n_i] \tag{14}$$

$$J_n^{i-1/2} = \frac{q\mu_n^{i-1/2}V_T}{h_{i-1}}[B(\Delta_n^{i-1/2})n_i - B(-\Delta_n^{i-1/2})n_{i-1}] \tag{15}$$

$$J_p^{i+1/2} = \frac{q\mu_p^{i+1/2}V_T}{h_i}[B(\Delta_p^{i+1/2})p_{i+1} - B(-\Delta_p^{i+1/2})p_i] \tag{16}$$

$$J_p^{i-1/2} = \frac{q\mu_p^{i-1/2}V_T}{h_{i-1}}[B(\Delta_p^{i+1/2})p_i - B(-\Delta_p^{i-1/2})p_{i-1}], \tag{17}$$

where

$$\Delta_n^{i+1/2} = \frac{\psi_{i+1} - \psi_i + \chi_{i+1} - \chi_i}{V_T} + \ln\frac{(\gamma_n N_C)_{i+1}}{(\gamma_n N_C)_i} \tag{18}$$

$$\Delta_n^{i-1/2} = \frac{\psi_i - \psi_{i-1} + \chi_i - \chi_{i-1}}{V_T} + \ln\frac{(\gamma_n N_C)_i}{(\gamma_n N_C)_{i-1}} \tag{19}$$

$$\Delta_p^{i+1/2} = \frac{\psi_{i+1} - \psi_i + \chi_{i+1} - \chi_i}{V_T} + \ln\frac{(\gamma_p N_V)_{i+1}}{(\gamma_p N_V)_i} + E_g^i - E_g^{i+1} \tag{20}$$

$$\Delta_p^{i-1/2} = \frac{\psi_{i-1} - \psi_i + \chi_{i-1} - \chi_i}{V_T} + \ln\frac{(\gamma_p N_V)_i}{(\gamma_p N_V)_{i-1}} + E_g^{i-1} - E_g^i \tag{21}$$

B is the Bernoulli function, γ is the ratio between the Fermi-Dirac and Boltzmann statistics.

In the local models α_n and α_p have been evaluated at the half-point between neighbouring nodes, since the field is piecewise continuous between nodes. The following interpolation formula was used for the avalanche generation:

$$G^i \approx \frac{h_{i-1}G^{i-1/2} + h_i G^{i+1/2}}{h_i + h_{i-1}}. \tag{22}$$

The DC solution was carried out through a Newton-Richardson coupled scheme. In the absence of avalanche ionization, the 1D model is not particularly critical with respect to a two-carrier homostructure model, although the use of Fermi-Dirac statistics coupled to a Newton scheme requires a rather cumbersome evaluation of the Jacobian if quadratic convergence is required.

From a numerical standpoint, the simulation of heterostructure APD's is made difficult by the presence of heterojunctions and very high fields: APD's work at very high inverse voltages (typically more than 50 V) thereby leading to convergence difficulties, mainly connected to the avalanche behaviour, which appear to be more serious than for homojunction structures. In order to avoid any numerical problems associated with truncation errors, the model was initially implemented in quadruple precision. Covergence at high bias was improved through the use of continuation techniques to provide an initial guess to the iterative process. High numerical accuracy is also required to evaluate the output currents of APD's, which show a dramatically wide dynamic range when going from the dark to the illuminated condition.

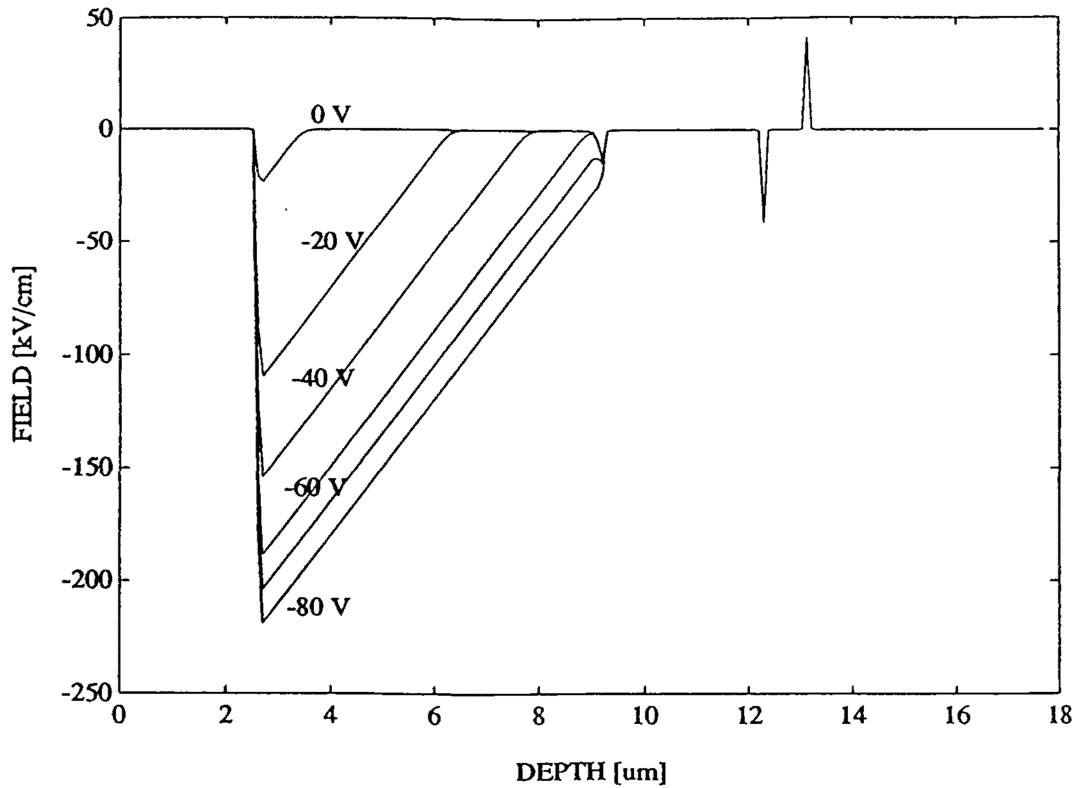

Figure 3: Field distribution in p^+-n photodiode as a function of reverse applied bias.

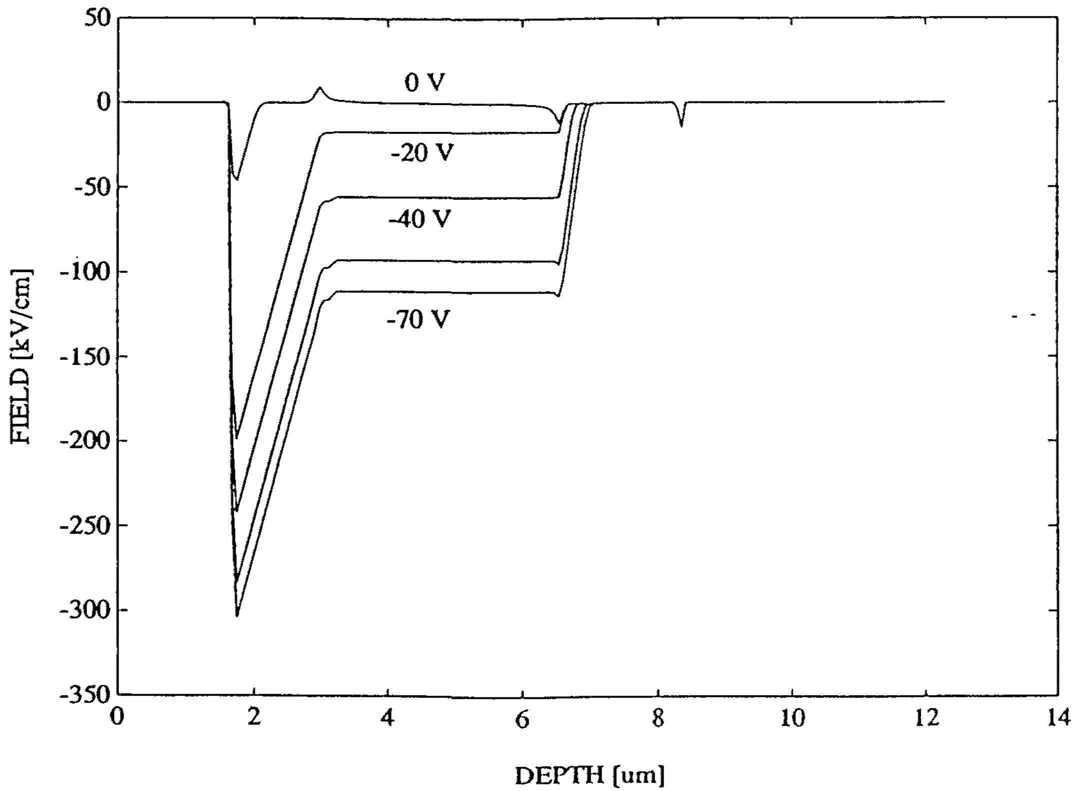

Figure 4: Field distribution in SAM-APD photodiode as a function of reverse applied bias.

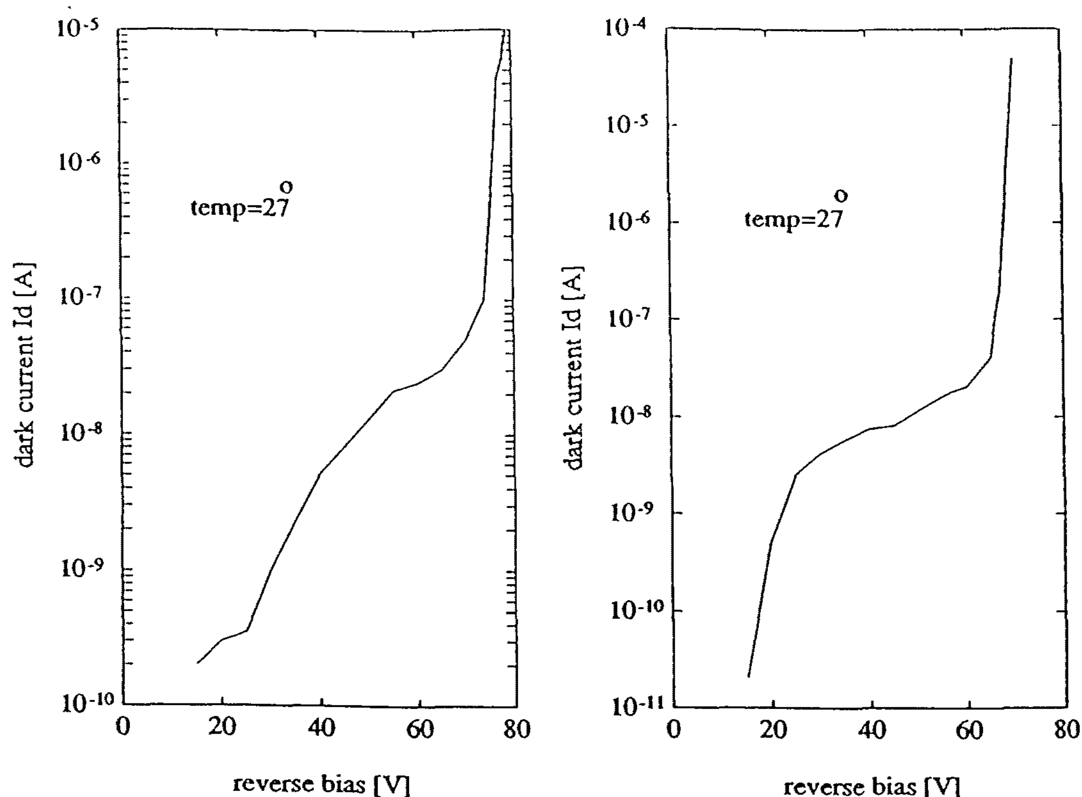

Figure 5: Dark currents of the p^+-n photodiode (left) and of the SAM-APD photodiode (right) as a function of reverse applied bias.

4 Results and discussion

Two typical, state-of-the-art APD's mesa structures were chosen for analysis: a $p^+ - n$ AlGaAs/GaAs photodiode (Fig.1) discussed in [3] and a Separated Absorption and Multiplication heterostructure APD (SAM-APD) (Fig.2) discussed in [4]. SAM-APD's are considered to provide the most sensitive photodetector structures for long wavelength optical communications, since it allows, with its InP/InGaAsP/InGaAs structure, an improvement of 1-3 dB sensitivity over Ge-APD's up to 2 Gbit/s [21, 13].

The different behaviour of the two structures appears in the electric field profile as a function of the reverse applied bias, shown in Fig.3 for the $p^+ - n$ APD and in Fig.4 for the SAM APD. In the first structure the electric field has a roughly triangular profile extending all over the depletion region. In this way, the regions wherein avalanche generation and optical absorption occur partly overlap, thereby giving rise to higher noise. Moreover, the larger avalanche region leads to higher transit times. Conversely, in the SAM-APD structure the superior properties allowed by the use of heterostructures clearly appears in the avalanche region (high energy gap material) being separated from the drift region wherein optical absorption occurs. As a consequence, noise decreases and the transit time is reduced. The plots of the dark currents for both structures, shown in Fig.5 at 300 K, confirm the better noise properties of SAM APD's. Finally, Fig.6 shows the behaviour of the avalanche ionization coefficients as a function of the reverse applied bias for the $p^+ - n$ diode (above) and the SAM APD (below); the result shown has been obtained with the Chynoweth model.

Acknowledgements. The authors wish to thank Prof. C.Naldi of Politecnico di Torino for helpful discussions.

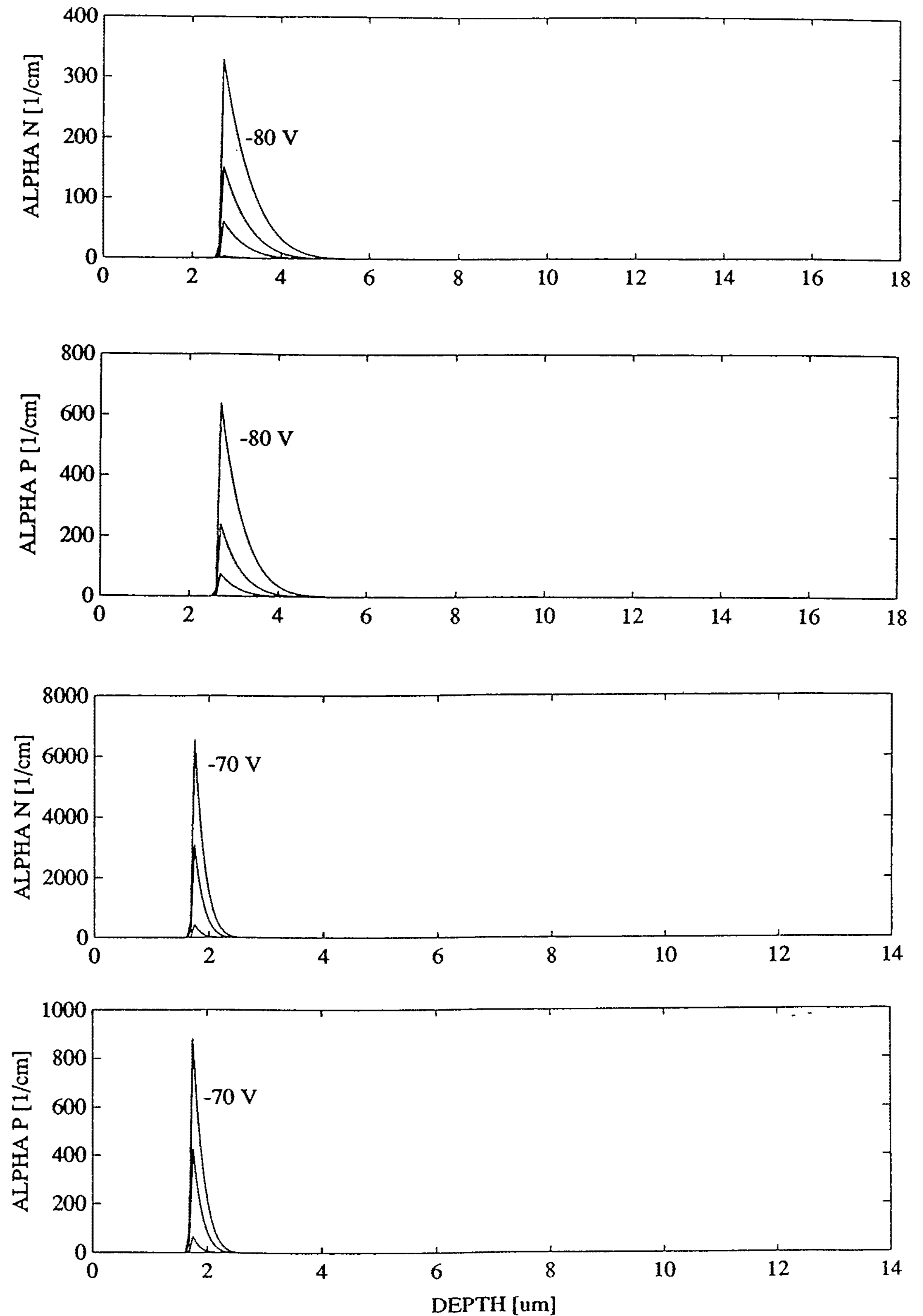

Figure 6: Spatial distribution of ionization coefficients according to the Chynoweth model as a function of applied reverse bias. From top row: p^+-n photodiode, α_n (above), α_p (below); SAM-APD photodiode, α_n (above), α_p (below).

References

[1] G.A.Baraff, "Distribution functions and ionization rates for hot electrons in semiconductors", *Phys. Rev.*, 128, p.2507, 1962

[2] D.M.Barry, S.P.Platt, C.M.Snowden, M.J.Howes and R.E.Miles, "Physical Modelling of GaAs Photodetectors", in G.Baccarani, M.Rudan, (Eds.), *Simulation of semiconductor devices and processes*, Vol.3, p.31, Tecnoprint, Bologna, 1988

[3] G.E.Bulman et al., "The determination of impact ionization coefficients in (100) gallium arsenide using avalanche noise and photocurrent multiplication measurements", *IEEE Trans. ED-32*, 11, p.2454, 1985

[4] M.Boulou et al., "InP/InGaAsP/InGaAs Avalanche photodiode with front illumination for optical fiber transmission at Gbit rates in the 1-1.6 μm wavelength region", *Proc. IOOC-ECOC'85*, p.549

[5] F.Capasso, "Physics of avalanche photodiodes", in *Semiconductors and Semimetals*, vol.22, p.2, Academic Press

[6] P.A.Childs, "Non-localised impact ionisation using a modified lucky drift theory", *J. Phys. C: Solid State Phys.* 20, L243, 1987

[7] A.G.Chynoweth, "Charge Multiplication Phenomena", in *Semiconductors and Semimetals*, vol.4, p.263, Academic Press

[8] M.Dentan and B. de Cremoux, "Numerical simulation of the nonlinear response of a p-i-n photodiode under high illumination", *Journal of Lightwave Technology*, Vol.8, No.8, p.1137, 1990

[9] R.P.Jindal, "A Monte Carlo simulation of a photodetection scheme employing noninstantaneous multiplication", *J. Appl. Phys.*, Vol.64, No.12, p.6845, 1988

[10] T.Lackner, "Avalanche multiplication in semiconductors: a modification of Chynoweth's law", *Solid-State Electronics*, Vol. 34, No.1, p.33, 1991

[11] M.S.Lundstrom and R.J.Schuelke, "Numerical analysis of heterostructure semiconductor devices", *IEEE Trans. ED-30*, No.9, p.1151, 1983

[12] A.H.Marshak, "Transport equations for highly doped devices and heterostructures", *Solid-State Electronics*, Vol.30, No.11, p.1089, 1987

[13] R.J.McIntyre, "Multiplication noise in uniform avalanche diodes", *IEEE trans. on Elect. Dev.*, ED-13, p.164, 1966

[14] C.Moglestue, "Monte-Carlo particle model study of a microwave photodetector", *IEE Proc.*, Part I, Vol.131, p.103

[15] T.P.Pearsall and M.A.Pollack, "Compound semiconductor photodiodes", in *Semiconductors and Semimetals*, vol.22, p.174, Academic Press

[16] S.Rakshit and R.Sarin, "Frequency responses of graded-bandgap low-noise avalanche photodiodes", *IEEE Trans. ED-32*, No.4, p.749, 1985

[17] A.A.R.Riad and R.E.Hayes, "Simulation studies in both the frequency and time domains of InGaAsP-InP avalanche photodetectors", *IEEE trans. on Elect. Dev.*, ED-27, p.1000, 1980

[18] H.Shichijo, K.Hess, G.E.Stillman, "Orientation dependence of ballistic electron transport and impact ionization", *Electron. Lett.*, Vol.16, No.6, p.208, 1980

[19] H.Shichijo and K.Hess, "Band structure dependent transport and impact ionization in GaAs", *Phys. Rev. B*, vol.23, No.8, p.4197, 1981

[20] W.Shockley, "Problems related to p-n junctions in silicon", *Solid-State Electronics*, 2, p.35, 1961

[21] K.Taguchi et al., "High-speed planar structure InP/InGaAsP/InGaAs avalanche photodiode grown by VPE", *IEEE Elect. Lett.*, 20, p.653, 1984

[22] J.E.Viallet and S.Mottet, "Heterojunction under Fermi-Dirac statistics: general set of equations and steady-state numerical methods", in J.J.H. Miller (Ed.), *Proceedings of NASECODE IV Conf.*, p.530, Boole Press, Dublin, 1985

[23] P.P.Webb et al., "Properties of avalanche photodiodes", *RCA Review*, 35, p.234, Jun. 1974

[24] P.A.Wolff, "Theory of electron multiplication in silicon and germanium", *Phys. Rev.*, 95, p.1415, 1954